A global view on how local muscular fatigue affects human performance

Márcio F. Goethel[a,b,c,1], Mauro Gonçalves[d], Cayque Brietzke[a,e], Adalgiso C. Cardozo[d], João P. Vilas-Boas[b,c], and Ulysses F. Ervilha[a,b,c]

[a]Laboratory of Physical Activity Sciences, School of Arts, Sciences, and Humanities, University of São Paulo, 03828-000 São Paulo, Brazil; [b]Centre of Research, Education, Innovation, and Intervention in Sport, Faculty of Sport, University of Porto, 4200-450 Porto, Portugal; [c]Porto Biomechanics Laboratory, University of Porto, 4200-450 Porto, Portugal; [d]Department of Physical Education, São Paulo State University, 13506-692 Rio Claro, Brazil; and [e]Exercise Psychophysiology Research Group, School of Arts, Sciences, and Humanities, University of São Paulo, 03828-000 São Paulo, Brazil

Edited by Peter L. Strick, University of Pittsburgh, Pittsburgh, PA, and approved July 10, 2020 (received for review April 28, 2020)

There is a growing interest in scientific literature on identifying how and to what extent interventions applied to a specific body region influence the responses and functions of other seemingly unrelated body regions. To investigate such a construct, it is necessary to have a global multivariate model that considers the interaction among several variables that are involved in a specific task and how a local and acute impairment affects the behavior of the output of such a model. We developed an artificial neural network (ANN)-based multivariate model by using parameters of motor skills obtained from kinematic, postural control, joint torque, and proprioception variables to assess the local fatigue effects of the abductor hip muscles on the functional profile during a single-leg drop landing and a squatting task. Findings suggest that hip abductor muscles' local fatigue produces a significant effect on a general functional profile, built on different control systems. We propose that expanded and global approaches, such as the one used in this study, have great applicability and have the potential to serve as a tool that guarantees ecological validity of future investigations.

artificial neural network | self-organizing feature maps | exercise | fatigue

By definition, muscle fatigue is the experience of the maximal force and power impairment (1). Interestingly, there is evidence that the duration of some sustained tasks is not limited by fatigue of the principal muscles (2). Since most daily-living activities involve submaximal force capacity using synergistic muscle groups, the onset of local fatigue may not reduce the ability to perform a given specific task (for example, either to support body weight during landing or to keep the body in a target position as still as possible). Furthermore, reduction in performance or failure in a task may not necessarily be caused by the main responsible muscle fatigue.

There is a growing body of literature showing that interventions applied to a specific anatomical region could influence an outcome and function of other, seemingly unrelated body regions (3–9). This phenomenon is called as regional interdependence (RI) and is defined as a concept that impairments seemingly unrelated in remote anatomical regions could be associated with a patient's primary condition (3). The RI model represents the musculoskeletal response of an interdependent process by which other systems may be entangled in evoking musculoskeletal changes. This involves an integrated and coordinated activation of multiple body systems (i.e., musculoskeletal, biopsychosocial, neurophysiological, etc.) (10). For example, localized muscle fatigue impairs movement coordination, proprioception, and muscle-reaction time (11, 12), which are imperative for postural balance maintenance (13, 14).

Several studies have shown the isolated effects of hip-abductor fatigue on postural control (15); torque distribution and dynamics of the lower limb joints (16); sense of joint position (17); and motor capacities involved in the drop-landing task (18). However, these analyses are fragmented and do not access the interdependence among the parameters affected by the hip-abductor muscles' local fatigue. Thereby, analyses made so far do not allow understanding of the effect of local fatigue in a general functional profile of the subject.

To investigate this construct, a global multivariate model is necessary, which considers the interaction of several variables involved in a motor task and how the hip-abduction force decrease, induced by muscle fatigue, affects the model output behavior.

From the 20th century up to nowadays, the inferences in biomedical research were mainly based on the use of traditional statistical procedures to test a hypothesis. The current surge of data and demands on more global analysis present new challenges and opportunities that are shifting data-analysis paradigms in many biomedical disciplines, including human-movement biomechanics. Data from human-movement experiments are heterogeneous, high-dimensional, and growing in volume, which make them not fitting to assumptions from traditional statistics. Advanced analytical techniques to assess informative features from these data and model underlying relationships that cannot be modeled with traditional statistical tools could increase the biomechanical research quality, as it has occurred in other areas of knowledge (i.e., speech recognition, disease detection, etc.) (19–22).

Artificial intelligence tools, more specifically the artificial neural networks (ANNs), have been widely used in science in general, including the human-movement sciences (23), in order to generate a more global understanding of multivariate phenomena. Indeed, such structures are able to access the linear and nonlinear relationships that possibly exist among the variables that construct the phenomenon, as well as to discover different patterns that allow identifying subpopulations that exhibit different types of behavior.

Significance

The human body is an organism with interdependent systems, where phenomena or interventions in a specific region can provoke responses in another apparently unrelated one. Localized muscle fatigue is characterized as a failure in the production of strength in a specific region caused by overuse. To investigate the global effect of this failure, access to interactions between different regions and systems is needed. In this work, we propose a global multivariate model based on artificial neural networks that produces as output a general functional profile, built from information from different control systems, which allows us to access the effects of local muscle fatigue on tasks that imply body performance as a single system.

Author contributions: M.F.G. and M.G. designed research; M.F.G. and U.F.E. performed research; M.F.G. and U.F.E. analyzed data; and M.F.G., C.B., A.C.C., J.P.V.-B., and U.F.E. wrote the paper.

The authors declare no competing interest.

This article is a PNAS Direct Submission.

[1]To whom correspondence may be addressed. Email: gbiomech@gmail.com.

First published August 4, 2020.

Our aim was to develop an ANN-based multivariate model using representative parameters of motor skills obtained from kinematic, postural control, joint torque, and proprioception variables to assess the local fatigue effects of the abductor hip muscles on the general functional profile in a single-leg drop landing and a squatting task.

Results

Behavior of the Variables Used to Compose the Model. Part of our results are expressed as the multiplication factor (MF) value of each condition that is multiplied by the constant value (as mean) of each variable. MF value represents the proportion of the amplitudes of the variables when obtained in the different conditions of the experiment. In the present study, the conditions investigated are prefatigue, during fatigue, and 20 min after the fatigue of the hip abductor muscles. Moreover, due to the large number of variables investigated (16 obtained during the unstable phase of the drop-landing task and 15 for the other investigated tasks), the graphs showing the MF values allow us to observe regional interdependence, since the MF values for kinetic and kinematic variables are plotted on the same graph. In Fig. 1, the behavior variables MF values obtained during the unstable phase of the squatting task can be visualized. The most visible changes occurred in the data obtained 20 min after the fatigue protocol, and they were observed in hip, knee, and ankle torque, showing increasing values. Squatting time and hip tilt showed similar results.

For the stable phase (Fig. 2) of the squatting task, it was possible to notice changes in variables related to postural control, such as the center of pressure (CoP) area, total CoP displacement, and CoP mean velocity. Visual differences of the MF values also occurred in the sense of position, where fatigue seemed to decrease absolute and variable errors.

Kinematic and kinetic variables obtained during the unstable and stable phases of the drop-landing task are shown, respectively, in Figs. 3 and 4. During the unstable phase, in the fatigue condition, the medio-lateral ground-reaction force, CoP area, CoP total displacement, and inverse dynamics of the ankle in the *z* and *y* axes presented MF values of 10 to 40% higher than those obtained in prefatigue conditions and 20 min after fatigue.

In the stable phase of the landing task (Fig. 4), the variables related to proprioception (variable and absolute error) presented increasing MF values (between 5% and 20%) in the order prefatigue, during fatigue, and 20 min after fatigue. The values obtained from inverse dynamics of the hip joint (in the *x* axis) presented higher MF values in the prefatigue condition, when compared to the other two conditions. The CoP total displacement and the area were greater in the condition 20 min after fatigue, followed by the condition fatigue and then prefatigue. The hip tilt also showed different MF values (between 10% and 40%) increasing in the following sequence: prefatigue, 20 min after fatigue, and during fatigue.

Classification Generated by ANN Structure. The results of the general functional profile classification of each subject in each condition are represented in Table 1 and are presented in two possible outcomes: changed (1) or unchanged (0).

To compare the ANN results of the binary categorical variable among the conditions prefatigue, fatigue, and 20 min postfatigue (24), the Cochran's Q test was applied. Next, the McNemar test was conducted to compare between pairs. Briefly, the effect sizes for both tests was calculated as previously suggested and classified as no effect (0 to 0.1), small effect (0.2 to 0.4), intermediate effect (0.5 to 0.7), and large effect (0.8 to ≥ 1) (25–27). For both tests, a significance level of $P < 0.05$ was accepted.

The results of the Cochran's Q test showed that there is a significant difference in the behavior of the general functional profile between the three conditions ($P < 0.001$; effect size = 0.20), and the McNemar test showed that the differences are between prefatigue and fatigue conditions ($P = 0.002$; effect size = 0.09), as well as between fatigue and postfatigue 20 min conditions ($P = 0.016$; effect size = 0.09). No difference was found between prefatigue and postfatigue 20 min ($P = 0.250$; effect size = 0.09).

Discussion

Considering that the human body is built based on interdependent systems, which include the sensorimotor system, motor-control impairments, even if acute and local, can generate deleterious consequences in the motor control of distant regions, possibly bringing harmful consequences for other segments and parts of the body-motor tasks. Such interdependence has been named the RI model (10). Moreover, pathological conditions start series of responses involving multiple body systems, not only at the musculoskeletal, but also at the neurophysiological, somatovisceral, and biopsychosocial levels (28, 29).

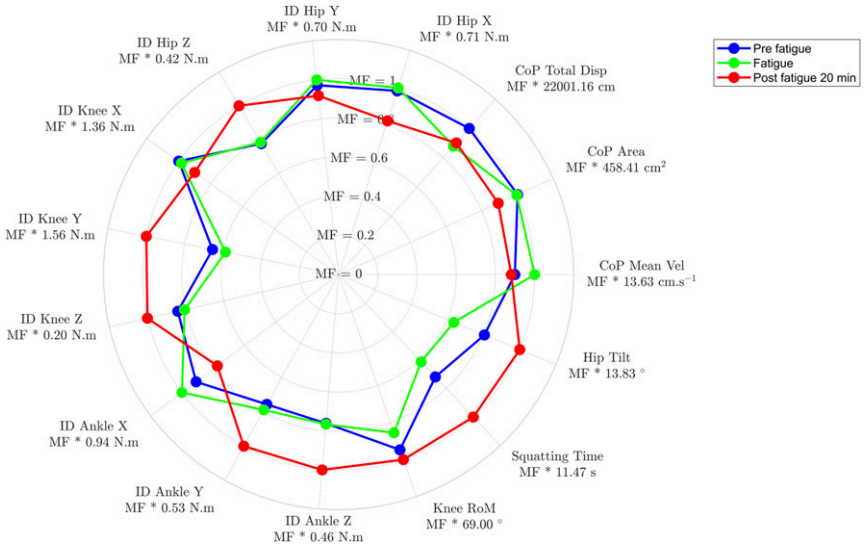

Fig. 1. MF for kinetic and kinematic variables obtained during the unstable phase of the squatting task. ID, inverse dynamics. For hip, knee, and ankle, X, Y, and Z mean adduction/abduction, extension/flexion, and rotation, respectively.

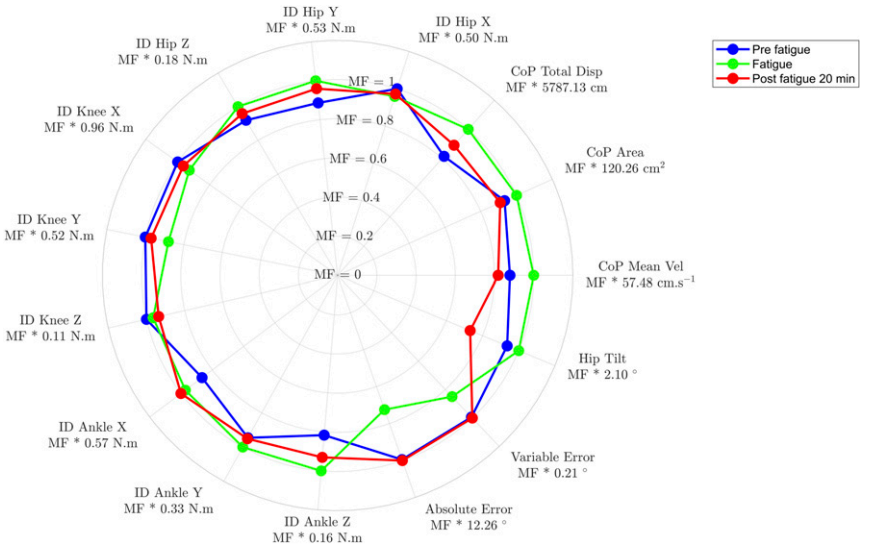

Fig. 2. MF for kinetic and kinematic variables obtained during the stable phase of the squatting task. ID, inverse dynamics. For hip, knee, and ankle, X, Y, and Z mean adduction/abduction, extension/flexion, and rotation, respectively.

As the concept of regional interdependence still consists of theory, for it to be validated experimentally it is necessary to demonstrate that the imbalance of one part of the body directly or indirectly influences other parts that are not directly related to it (9, 30–34). Our results, based on acute and local muscle fatigue, point to the existence of interdependence among the articulated segments of the pelvis and the lower-limb segments. We have shown that in a unipodal landing and in a task of bringing a joint (not directly involved with the fatigued muscles) to a target position, muscle fatigue of the abductor muscles of the hip affects variables related to strength and proprioception, not only at the hip, but also in other segments of the lower limb.

Interdependence between left and right hip joints in postural control has already been shown (15). Specifically, it was found that unipodal postural control is altered either by fatigue of the hip abductor muscles on the support side or in the abductor muscles of the contralateral hip, suggesting that, in addition to local muscle fatigue, changes in the central nervous system might have taken place.

In a very interesting study with an ecological appeal for athletes (16), volunteers were asked to jump off a platform, perform unipodal landing, and then perform either a side-step cut, a straight vertical jump, or continue to run from that point. The results showed that, regardless of the maneuver, due to hip-abductor fatigue, during the weight acceptance of the stance phase, the knee angle at initial ground contact was more adducted, the knee underwent greater range of motion (RoM) into abduction, and there was a greater internal knee adductor moment.

Fatigue of hip-abductor muscles has also been related to changes in proprioception. There is a study reporting that the hip-position sense was significantly affected by fatigue, as indicated by an increased relative error of 0.78, in the joint-position sense, toward abduction (17). Changes in the joint positioning (during single-leg landing) of the lower limb due to fatigue of the hip abductors was also shown (18). According to Patrek et al. (18), fatiguing processes may affect negatively the hip-abduction and knee-abduction angle. The authors also observed that the peak of external knee adduction was decreased around 27%, while the peak of hip-adduction moment was decreased around 24% in the postfatigue landing trial.

In contrast with the finding of Arvin et al. (17), our results showed that the position sense, represented by absolute and variable error, presents smaller error values during the fatigue condition. The difference between our findings and those of the authors cited above may be because we measured the position sense of a joint not directly involved with local fatigue, unlike what was done by Arvin et al. (17), who measured the position sense of the hip, which was the joint directly involved with the fatigue of the hip abductors.

Moreover, it is important to emphasize that the alterations found are interrelated. For example, when observing a decrease in the capacities of postural control, it is common to observe an increase in the articular moments in the lower limb. Furthermore, an increase in the hip tilt certainly changes the abilities of postural control. In the same way, we can infer that a joint exposed to greater internal torques has its sense of position affected.

By observing the interdependence between all of the systems investigated in the present study, it is possible to identify that all changes observed lead to a significant alteration ($P < 0.001$) of the general functional profile constructed by the ANN structure. It is possible to observe that, due to the application of the fatigue protocol, 76.9% of the subjects suffered a significant change in their general functional profile in relation to the prefatigue condition ($P = 0.002$) and that 70% of them had a significant recovery after 20 min ($P = 0.016$). Furthermore, it was observed that the state after the 20-min recovery period did not present a significant difference from the prefatigue condition ($P = 0.250$).

Researchers suggest that this expanded and global approach produces more ecological understanding and result in positive findings, especially when it comes to understanding and treating mechanisms of injury or illness. Trials that uses a multimodal analysis approach sustained by RI concepts, for instance, have shown to be effective (5, 35–37).

In conclusion, our findings pointed out that local fatigue of the hip-abductor muscles produces a significant effect on a general functional profile, built on different control systems, and that this effect may change between the different systems. It also can be applicable for most of the volunteers of the present study. Finally, we suggest that expanded and global approaches such as the one used in this study have great applicability and have the potential to serve as a tool that guarantees ecological validity of future investigations.

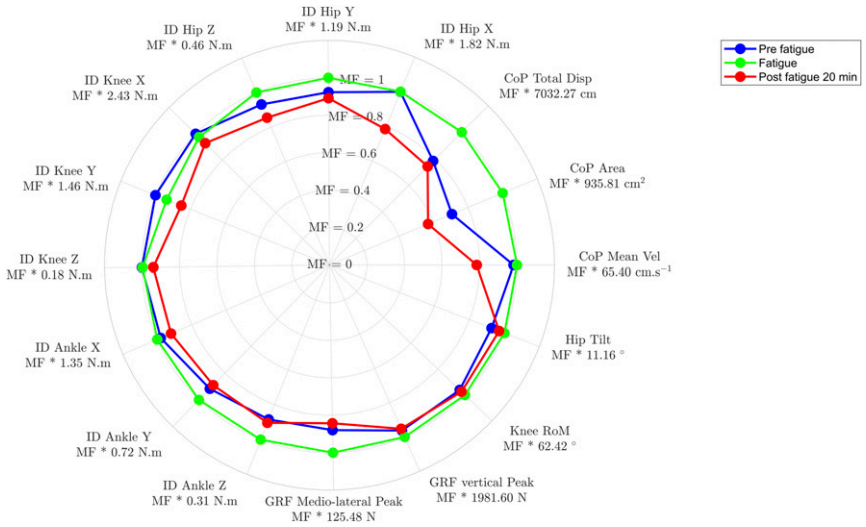

Fig. 3. MF for kinetic and kinematic variables obtained during the unstable phase of the drop-landing task. ID, inverse dynamics. For hip, knee, and ankle, X, Y, and Z mean adduction/abduction, extension/flexion, and rotation, respectively.

Materials and Methods

Sample. Thirteen sedentary women (38) (21.1 ± 2.1 y of age, 1.60 ± 0.06 m in height, and 56.5 ± 14.5 kg in body mass) voluntarily took part in this study. Exclusion criteria consisted of pain or surgery in the lower limbs, inability to remain on unipodal support during the execution of the proposed tasks, recent injuries, decompensated hypertension, or heart problems. This study was approved by the ethics committee of São Judas Tadeu University (registry n.93/11), and the procedures were carried out in accordance with the Declaration of Helsinki. After receiving all information about the data-collection protocols so that they could participate in the study, all participants gave their duly signed informed consent forms.

Experimental Protocol.

Familiarization with the target knee angle. During the training phase, subjects performed unipodal squatting movements with a break at the end to have visual feedback on a computer screen. Subjects had to fit knee, trochanter, and ankle over three fixed points displayed on the screen, imposing positioning the knee joint at a 35° of flexion (considering total extension equal to 0°). Further, verbal feedback was given to the subjects in a nominal order as "correct" or "incorrect" joint positioning. The memorization was trained by keeping the knee in the target position for 5 s. To conclude the training phase, the volunteer was considered to be familiar when able to locate the target angle three consecutive times. During the whole experimental protocol, subjects performed the tasks with their dominant limb to ensure control regarding postural control and sense of position.

Fatigue protocol. The fatigue-inducing protocol consisted of performing hip abduction (concentric) and adduction (eccentric) movements at a frequency of 1 Hz, marked by a metronome, from the lateral decubitus position, resisted with a mass equivalent to 5% body weight attached to the ankle. Volunteers were instructed to perform as many movements as possible and received constant standardized verbal encouragement. Briefly, the encouragements were standardized for all subjects, as the same investigator performed it by using standardized words during the whole test. The test of all volunteers was managed by the same evaluator. When the volunteer failed to repeat the movements, the maximal voluntary isometric contraction of hip abduction was immediately tested by using an isokinetic dynamometer, Biodex System 4, in order to verify if there was a decrease of at least 50% in torque peak (39, 40). Once fatigue was observed, the volunteer was instructed to perform the tasks of squatting or drop landing, with no relevant resting period. The task-execution order was randomized. After the first task was performed, the volunteer returned to the fatigue protocol

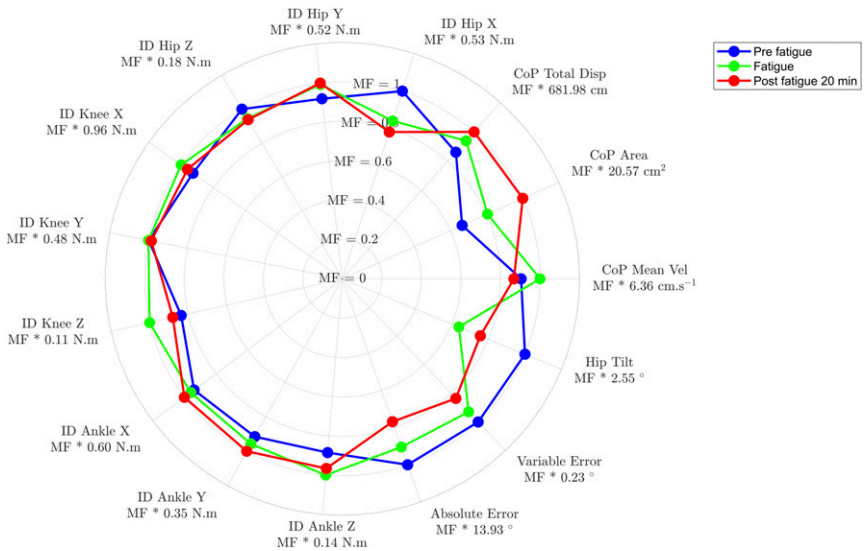

Fig. 4. MF for kinetic and kinematic variables obtained during the stable phase of the drop-landing task. ID, inverse dynamics. For hip, knee, and ankle, X, Y, and Z mean adduction/abduction, extension/flexion, and rotation, respectively.

Table 1. Results from ANN classification

	Prefatigue	Fatigue	Postfatigue 20 min
Subject 01	0	1	1
Subject 02	0	1	0
Subject 03	0	0	0
Subject 04	0	1	0
Subject 05	0	1	0
Subject 06	0	0	0
Subject 07	0	1	0
Subject 08	0	0	0
Subject 09	0	1	1
Subject 10	0	1	0
Subject 11	0	1	0
Subject 12	0	1	1
Subject 13	0	1	0

until the fatigue condition was checked again, so that the second task was carried out.

Squatting task. Immediately after performing three unipodal squat movements, the volunteer was instructed to position the knee joint at the predetermined target angle and thus remain (as still as possible) for 3 s. This procedure was performed under three conditions—namely, before the application of the fatigue protocol (prefatigue), immediately after the induction of fatigue (fatigue), and 20 min after fatigue protocol (postfatigue 20 min).

Drop-landing task. Volunteers were instructed to remain in unipodal support on a platform 30 cm high. As soon as authorized, they leaped forward in order to land on unipodal support over a force platform placed immediately in front of the support platform. They were instructed to position the knee joint in the predetermined target position immediately after landing and remain as still as possible for 3 s. This procedure was repeated three times in each of the following conditions: prefatigue, fatigue, and 20 min postfatigue.

Data collection and processing. In order to acquire kinematic data during the squatting and drop-landing tasks at a frame rate of 250 frames per second, seven T10 (Vicon) cameras were used. For the motion reconstruction, basic reflective markers (Vicon) were fixed bilaterally according to the PluginGait model for the whole body (Vicon). The volunteers performed the squatting and the drop-landing tasks on an AMTI model OR6-2000 force platform, allowing us to acquire the kinetic data of ground reaction (sampling frequency = 1,500 Hz). Kinematic and kinetic data were acquired synchronously by the Vicon Nexus software (Vicon).

The optimal cutoff frequency for signal filtering was found by using the residual analysis (41), wherein the signal of the kinematic data was filtered with a recursive fourth-order low-pass Butterworth filter with the cutoff frequency of 6 Hz and the kinetic data with a recursive fourth-order low-pass Butterworth filter with the cutoff frequency of 95 Hz.

All data were processed and analyzed through specific routines developed in Matlab (Version 8.5.0.197613; MathWorks, Inc.).

Data Analysis.

Unstable and stable phase of the tasks. Initially, based on the angulation of knee flexion, the signals were divided into two phases: unstable phase and stable phase. The unstable phase comprised the time between the beginning of the task and the beginning of the stable phase. The stable phase, however, was defined as the 1-s time period which presented the lesser variation of the angular position within the time period of 3 s in which the volunteer tried to remain with the knee flexed in the target angular position. The beginning of the stable phase was determined by using the approximated generalized likelihood ratio (AGLR) method.

AGLR (42–44) is based on statistical testing of the null hypotheses H_0 and the alternate hypothesis H_1 describing the statistical properties of series of knee flexion angle samples $x_1, x_2, \ldots, x_k$. H_0 indicates no change within the analyzed time window of the knee flexion angle signal, and H_1 indicates that change has occurred in the tested time window of the signal. Two hypotheses were tested by using a log-likelihood ratio test $g(n)$:

$$g(n) = \ln\left(\prod_{n=1}^{k} \frac{p_1(x_n)|H_1}{p_0(x_n)|H_0}\right) \gtrless h, \quad [1]$$

where *ln* represents natural logarithm, $x(n)$ represents series of knee flexion angle samples, and p_1 and p_0 represent probability density functions associated with hypotheses H_1 and H_0, respectively. When log-likelihood $g(n)$ is higher than preset threshold "h," then the hypothesis H_1 is accepted, meaning that signal change is detected. The AGLR algorithm performs hypothesis testing in a sliding window of size L, over the series of knee flexion angle data. The log-likelihood ratio is calculated from L samples for every window epoch. The signal stability is detected (smaller $g(n)$) when the hypothesis H_0 is considered valid, which means that no signal change is detected, allowing us to estimate the onset of the stable phase, with a duration of 1 s, found by maximizing likelihood estimators for each sample from the last window position. For the AGLR algorithm, the window size was set at $L = 0.032$ s (eight samples), and the detection threshold was set at $h = 14$ (45).

Variables Definition.

Knee RoM. During the squatting and drop-landing tasks, the knee RoM was calculated as the difference between the highest and the lowest knee flexion angle value obtained during the unstable phase.

Squatting time. Squatting time consisted of the time period between the beginning of the squatting task and the beginning of the stable phase.

Absolute error. The absolute error (*AE*) is the error measure of the position sense based on the target angulation and was calculated during the stable phase by using the following equation:

$$AE = \frac{\sum_{i=1}^{n} |x_i - A|}{n}, \quad [2]$$

where x_i indicates the knee flexion angle in the i sample; A indicates the target knee flexion angle; and n refers to the number of samples.

Variable error. The variable error (*VE*) is the error measure of the position sense based on the variability of the maintained angle and was calculated during the stable phase by using the following equation:

$$VE = \sqrt{\frac{\sum_{i=1}^{n} (x_i - \overline{x})^2}{n}}, \quad [3]$$

where x_i indicates the knee flexion angle of the volunteer in the i sample; $\overline{x}$ indicates the average of the angular positions maintained during the stable phase; and n refers to the number of samples.

Hip tilt. Hip tilt (*HT*) consists of the leveling of the anterior superior iliac spines, calculated by using the following equation:

$$HT_i = \tan^{-1}\left(\frac{LasiZ_i - RasiZ_i}{LasiY_i - RasiY_i}\right), \quad [4]$$

where *LasiZ* means the position of the left antero-superior iliac spine on the vertical axis in the i sample; *RasiZ* means the position of the right antero-superior iliac spine on the vertical axis in the i sample; *LasiY* means the position of the left antero-superior iliac spine on the medio-lateral axis in the i sample; and *RasiY* means the position of the right antero-superior iliac spine on the medio-lateral axis in the i sample.

The difference between the maximum and the minimum value was calculated in both phases of both tasks.

Ground reaction forces and CoP. From the kinetic data acquired using the force platform, ground reaction force (GRF) on the medio-lateral and vertical axes during the unstable phase of the drop-landing task were analyzed.

The CoP was calculated for the antero-posterior and medio-lateral axes from Eqs. **5** and **6**, respectively, as described below:

$$CoP_{ap} = -\frac{M_y}{F_z}, \quad [5]$$

$$CoP_{ml} = \frac{M_x}{F_z}, \quad [6]$$

where M_y is the medio-lateral moment, M_x is the antero-posterior moment, and F_z is the GRF in the vertical axis.

The total displacement of the CoP ($CoP_{\text{TotalDisp}}$) is calculated as the sum of the resultant displacements of the CoP in the antero-posterior and medio-lateral directions and was accessed through Eq. **7**:

$$CoP_{TotalDisp} = \sum_{i=1}^{n}\left(\left|\sqrt{CoP_{ap_{(i+1)}}^2 + CoP_{ml_{(i+1)}}^2} - \sqrt{CoP_{ap_{(i)}}^2 + CoP_{ml_{(i)}}^2}\right|\right). \quad [7]$$

The mean velocity of CoP excursion (CoP_{MeanVel}) was calculated as the

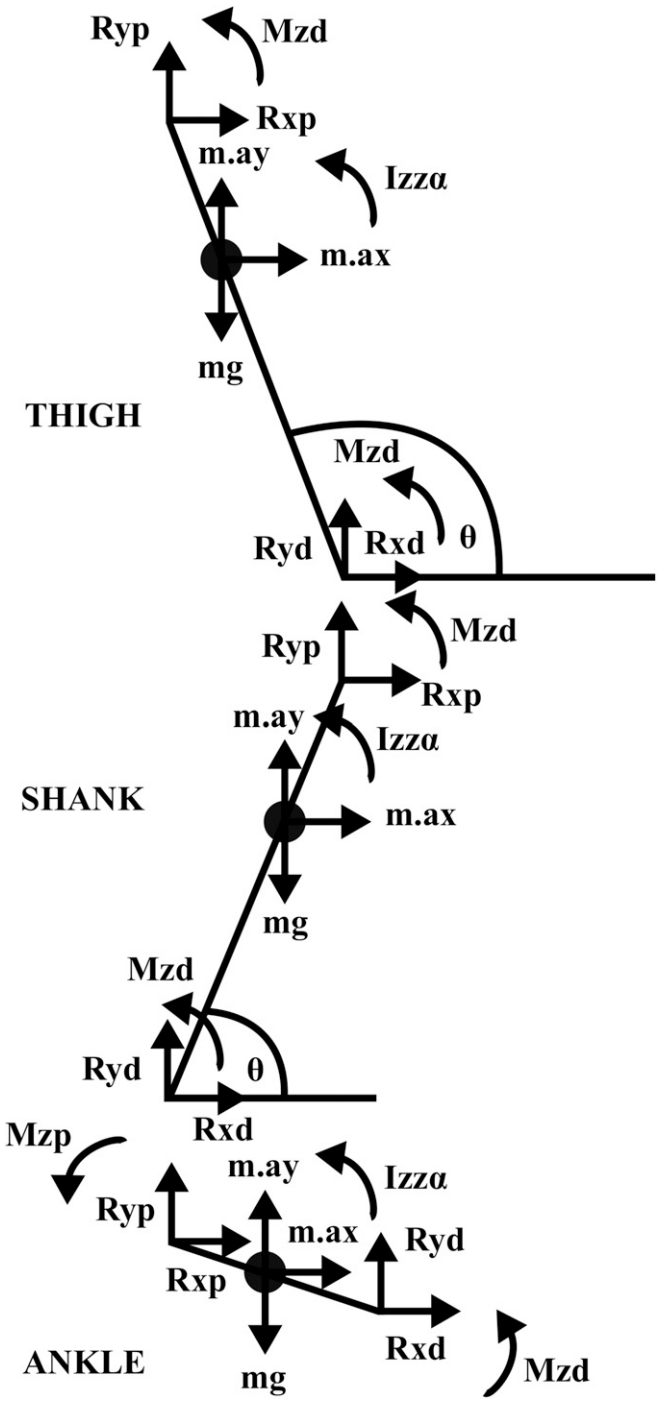

Fig. 5. Graphical representation of the lower-limb link-segment model.

resultant displacements of the CoP in the antero-posterior and medio-lateral directions in function of time, obtained through Eq. **8**.

$$CoP_{MeanVel} = \left(\sum_{i=1}^{n} \left(\frac{\left(\left| \sqrt{CoP_{ap_{(i+1)}}^2 + CoP_{ml_{(i+1)}}^2} - \sqrt{CoP_{ap_{(i)}}^2 + CoP_{ml_{(i)}}^2} \right| \right)}{(1 \div fs)} \right) \right) \div n, \quad [8]$$

where *fs* is the acquisition frequency of the force platform (1,500 Hz).

The measure of CoP area consists of the area of the 95% prediction ellipse, and the calculation was conduct according to Chew (46).

The parameters from the CoP excursion were calculated for both phases in both tasks.

Articular torque distribution. To calculate the triaxial joint moment in the ankle (ID Ankle *x*, *y*, and *z*), knee (ID Knee *x*, *y*, and *z*), and hip (ID Hip *x*, *y*, and *z*), the inverse-dynamics approach was used. The Newton–Euler equations (Eqs. **9** and **14**) described the behavior of a mathematical model as a link-segment model (Fig. 5). Briefly, the joint moments *x*, *y*, and *z* means adduction/abduction, extension/flexion, and rotation, respectively.

Through the Newton equation (Eq. **9**), it is possible to determine the joint reaction forces by calculating the sum of the horizontal forces in the antero-posterior (Eq. **10**), medial-lateral (Eq. **11**), and vertical (Eq. **13**) axes.

$$\sum F_{x|y} = m \cdot a_{x|y}, \quad [9]$$

$$R_{xp} = m \cdot a_x - R_{xd} \ldots, \quad [10]$$

$$R_{yp} = m \cdot a_y - R_{yd} \ldots, \quad [11]$$

where *P* is proximal, *d* is distal joint, and $a_{x|y}$ is acceleration of segment center of mass (CoM), in the antero-posterior or medial-lateral direction; e.g., *d* is the force platform when *p* is the ankle.

$$\sum F_z = m \cdot a_z, \quad [12]$$

$$R_{zp} = m \cdot a_z + m \cdot g - R_{zd}. \quad [13]$$

By applying the Euler equation and using the inertial parameters, it is possible to determine the joint moments by calculating the sum of moments as shown in Eqs. **14**–**16**.

$$\sum M_{\dot{x}|\dot{y}|\dot{z}} = I_{x|y|z} \cdot \alpha_{x|y|z}, \quad [14]$$

$$M_{xp|yp|zp} = I_{x|y|z} \cdot \alpha_{x|y|z} - M_{xd|yd|zd} - R_{xp|yp} \cdot r_p \cdot \sin(\theta) + R_{zp} \cdot r_p \cdot \cos(\theta) + R_{xd|yd} \cdot r_d \cdot \sin(\theta) - R_{zd} \cdot r_d \cdot \cos(\theta), \quad [15]$$

where r_p is the distance from segment CoM to the proximal joint; and θ is the angle of segment to the right-hand horizontal.

Using the motion coordinates, we obtain:

$$M_{\dot{x}p|\dot{y}p|\dot{z}p} = I_{x|y|z} \cdot \alpha_{x|y|z} - M_{\dot{x}d|\dot{y}d|\dot{z}d} - R_{xp|yp} \cdot (Z_p - Z_{CoM}) + R_{zp} \cdot \left(x \middle| y_{CoM} - x \middle| y_p \right) + R_{xd|yd} \cdot (Z_{CoM} - Z_d) - R_{zd} \cdot \left(x \middle| y_p - x \middle| y_{CoM} \right) \ldots, \quad [16]$$

where (x_{com}, y_{com}, z_{com}) are the coordinates of the center of mass of the segment, (x_p, y_p, z_p) are the coordinates of the proximal joint, and (x_d, y_d, z_d) are the coordinates of the distal joint.

ANN structure development and training. The structure of ANN used was the Self Organizing Feature Maps (SOFMs) (47, 48), which simulate how cells in the mammalian cerebral cortex organize themselves in a highly structured way, resulting in regions of the brain specifically trained in the sensory processing of signals such as vision, hearing, motor control, language, etc. (48), thus organizing the information in a spatial manner.

The SOFM is a network structure for working with unsupervised learning that learns to sort the input vectors according to how they are grouped in the input space. They differ from the competitive layers in which neighboring neurons in the self-organization map learn only to recognize the neighboring sections of the input space, so they learn both the distribution and the topology of the input vectors in which they are trained. This type of structure has already been widely applied to biomechanical analysis (49–51).

The learning algorithm used was the Batch Weight/Bias Rules, where each weight and bias is updated according to their learning function after each epoch (a passage through the set of input vectors). A 2,000-epochs limit was established for network training. The structure (Fig. 6) consisted of 61 variables in the input space (15 variables from the unstable and 15 from the stable

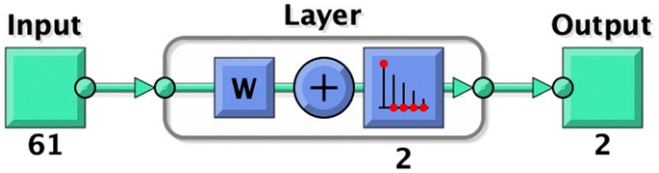

Fig. 6. Self-organizing feature maps structure. Input: 61 kinetic and kinematic variables. Output: "0," no change, or "1," change in the general functional profile.

phase of the squatting task; and 16 and 15 variables, respectively, from the unstable and the stable phase of the drop-landing task) for each subject and in three conditions, prefatigue, fatigue, and 20 min postfatigue, covering the behavior of lower-limb kinematics, postural control, proprioception, joint-torque distribution, and landing-involved capacities. The output space consisted of a binary classification composed of "0" or "1," indicating, respectively, "no change" and "change" in the general functional profile.

Data Availability. The data are available on Figshare as a public dataset under the CC BY 4.0 license (https://doi.org/10.6084/m9.figshare.12514289) (52).

ACKNOWLEDGMENTS. The present study was supported by the Brazilian government through its Coordination for the Improvement of Higher Education Personnel–"Coordenação de Aperfeiçoamento de Pessoal de Nível Superior" Grant 88882.315726/2019-01.

1. S. C. Gandevia, Spinal and supraspinal factors in human muscle fatigue. *Physiol. Rev.* **81**, 1725–1789 (2001).
2. R. M. Enoka, J. Duchateau, Muscle fatigue: What, why and how it influences muscle function. *J. Physiol.* **586**, 11–23 (2008).
3. R. S. Wainner, J. M. Whitman, J. A. Cleland, T. W. Flynn, Regional interdependence: A musculoskeletal examination model whose time has come. *J. Orthop. Sports Phys. Ther.* **37**, 658–660 (2007).
4. R. E. Boyles *et al*., The short-term effects of thoracic spine thrust manipulation on patients with shoulder impingement syndrome. *Man. Ther.* **14**, 375–380 (2009).
5. J. A. Cleland, J. D. Childs, M. McRae, J. A. Palmer, T. Stowell, Immediate effects of thoracic manipulation in patients with neck pain: A randomized clinical trial. *Man. Ther.* **10**, 127–135 (2005).
6. L. L. Currier *et al*., Development of a clinical prediction rule to identify patients with knee pain and clinical evidence of knee osteoarthritis who demonstrate a favorable short-term response to hip mobilization. *Phys. Ther.* **87**, 1106–1119 (2007).
7. P. E. Mintken *et al*., Some factors predict successful short-term outcomes in individuals with shoulder pain receiving cervicothoracic manipulation: A single-arm trial. *Phys. Ther.* **90**, 26–42 (2010).
8. R. B. Souza, C. M. Powers, Differences in hip kinematics, muscle strength, and muscle activation between subjects with and without patellofemoral pain. *J. Orthop. Sports Phys. Ther.* **39**, 12–19 (2009).
9. J. B. Strunce, M. J. Walker, R. E. Boyles, B. A. Young, The immediate effects of thoracic spine and rib manipulation on subjects with primary complaints of shoulder pain. *J. Manual Manip. Ther.* **17**, 230–236 (2009).
10. D. G. Sueki, J. A. Cleland, R. S. Wainner, A regional interdependence model of musculoskeletal dysfunction: Research, mechanisms, and clinical implications. *J. Manual Manip. Ther.* **21**, 90–102 (2013).
11. K. Häkkinen, P. V. Komi, Effects of fatigue and recovery on electromyographic and isometric force- and relaxation-time characteristics of human skeletal muscle. *Eur. J. Appl. Physiol. Occup. Physiol.* **55**, 588–596 (1986).
12. H. B. Skinner, M. P. Wyatt, J. A. Hodgdon, D. W. Conard, R. L. Barrack, Effect of fatigue on joint position sense of the knee. *J. Orthop. Res.* **4**, 112–118 (1986).
13. D. A. Winter, Human balance and posture control during standing and walking. *Gait Posture* **3**, 193–214 (1995).
14. F. B. Horak, Postural orientation and equilibrium: What do we need to know about neural control of balance to prevent falls? *Age Ageing* **35** (suppl. 2), ii7-ii11 (2006).
15. N. Sarabon, K. Hirsch, Z. Majcen, The acute effects of hip abductors fatigue on postural balance. *J. Sports Sci. Med.* **5**, 5–9 (2016).
16. C. F. Geiser, K. M. O'Connor, J. E. Earl, Effects of isolated hip abductor fatigue on frontal plane knee mechanics. *Med. Sci. Sports Exerc.* **42**, 535–545 (2010).
17. M. Arvin *et al*., Effects of hip abductor muscle fatigue on gait control and hip position sense in healthy older adults. *Gait Posture* **42**, 545–549 (2015).
18. M. F. Patrek, T. W. Kernozek, J. D. Willson, G. A. Wright, S. T. Doberstein, Hip-abductor fatigue and single-leg landing mechanics in women athletes. *J. Athl. Train.* **46**, 31–42 (2011).
19. K. Kalyan, B. Jakhia, R. D. Lele, M. Joshi, A. Chowdhary, Artificial neural network application in the diagnosis of disease conditions with liver ultrasound images. *Adv. Bioinformatics* **2014**, 708279 (2014).
20. F. Amato *et al*., Artificial neural networks in medical diagnosis. *J. Appl. Biomed.* **11**, 47–58 (2013).
21. S. Kurogi, Speech recognition by an artificial neural network using findings on the afferent auditory system. *Biol. Cybern.* **64**, 243–249 (1991).
22. A. Nichie, G. A. Mills, Voice recognition using artificial neural networks and Gaussian mixture models. *Int. J. Eng. Sci. Technol.* **5**, 1120–1129 (2013).
23. E. Halilaj *et al*., Machine learning in human movement biomechanics: Best practices, common pitfalls, and new opportunities. *J. Biomech.* **81**, 1–11 (2018).
24. I. C. H. Smith, D. J. Newham, Fatigue and functional performance of human biceps muscle following concentric or eccentric contractions. *J. Appl. Physiol.* **102**, 207–213 (2007).
25. R. C. Serlin, J. Carr, L. A. Marascuilo, A measure of association for selected nonparametric procedures. *Psychol. Bull.* **92**, 786–790 (1982).
26. K. J. Berry, J. E. Johnston, P. W. Mielke Jr., An alternative measure of effect size for Cochran's Q test for related proportions. *Percept. Mot. Skills* **104**, 1236–1242 (2007).
27. W. Lenhard, A. Lenhard, Calculation of effect sizes (Psychometrica, Dettelbach, Germany, 2019).
28. C. R. Chapman, R. P. Tuckett, C. W. Song, Pain and stress in a systems perspective: Reciprocal neural, endocrine, and immune interactions. *J. Pain* **9**, 122–145 (2008).
29. B. S. Mcewen, J. C. Wingfield, What is in a name? Integrating homeostasis, allostasis and stress. *Horm. Behav.* **57**, 105–111 (2011).
30. J. E. Bialosky, M. D. Bishop, S. Z. George, Regional interdependence: A musculoskeletal examination model whose time has come. *J. Orthop. Sports Phys. Ther.* **38**, 159–160, author reply 160 (2008).
31. J. D. Dishman, B. M. Cunningham, J. Burke, Comparison of tibial nerve H-reflex excitability after cervical and lumbar spine manipulation. *J. Manipulative Physiol. Ther.* **25**, 318–325 (2002).
32. S. Z. George, M. D. Bishop, J. E. Bialosky, G. Zeppieri Jr., M. E. Robinson, Immediate effects of spinal manipulation on thermal pain sensitivity: An experimental study. *BMC Musculoskelet. Disord.* **7**, 68 (2006).
33. M. D. Smith, A. Russell, P. W. Hodges, Do incontinence, breathing difficulties, and gastrointestinal symptoms increase the risk of future back pain? *J. Pain* **10**, 876–886 (2009).
34. B. Vicenzino, J. A. Cleland, L. Bisset, Joint manipulation in the management of lateral epicondylalgia: A clinical commentary. *J. Manual Manip. Ther.* **15**, 50–56 (2007).
35. J. M. Fritz, G. P. Brennan, Preliminary examination of a proposed treatment-based classification system for patients receiving physical therapy interventions for neck pain. *Phys. Ther.* **87**, 513–524 (2007).
36. M. J. Walker *et al*., The effectiveness of manual physical therapy and exercise for mechanical neck pain: A randomized clinical trial. *Spine* **33**, 2371–2378 (2008).
37. J. A. Cleland *et al*., Examination of a clinical prediction rule to identify patients with neck pain likely to benefit from thoracic spine thrust manipulation and a general cervical range of motion exercise: Multi-center randomized clinical trial. *Phys. Ther.* **90**, 1239–1250 (2010).
38. C. L. Craig *et al*., International physical activity questionnaire: 12-country reliability and validity. *Med. Sci. Sports Exerc.* **35**, 1381–1395 (2003).
39. C. Jacobs, T. L. Uhl, M. Seeley, W. Sterling, L. Goodrich, Strength and fatigability of the dominant and nondominant hip abductors. *J. Athl. Train.* **40**, 203–206 (2005).
40. E. J. Bisson, D. McEwen, Y. Lajoie, M. Bilodeau, Effects of ankle and hip muscle fatigue on postural sway and attentional demands during unipedal stance. *Gait Posture* **33**, 83–87 (2011).
41. D. A. Winter, *Biomechanics and Motor Control of Human Movement*, (Wiley, New York, NY, ed. 4, 2009).
42. G. Staude, C. Flachenecker, M. Daumer, W. Wolf, Onset detection in surface electromyographic signals: A systematic comparison of methods. *J. Appl. Signal Process.* **2**, 67–81 (2001).
43. G. Staude, W. Wolf, Objective motor response onset detection in surface myoelectric signals. *Med. Eng. Phys.* **21**, 449–467 (1999).
44. G. H. Staude, Precise onset detection of human motor responses using a whitening filter and the log-likelihood-ratio test. *IEEE Trans. Biomed. Eng.* **48**, 1292–1305 (2001).
45. D. Roetenberg, J. H. Buurke, P. H. Veltink, A. Forner Cordero, H. J. Hermens, Surface electromyography analysis for variable gait. *Gait Posture* **18**, 109–117 (2003).
46. V. Chew, Confidence, prediction, and tolerance regions for the multivariate normal distribution. *J. Am. Stat. Assoc.* **61**, 605–617 (1966).
47. T. Kohonen, Self-organized formation of topologically correct feature maps. *Biol. Cybern.* **43**, 59–69 (1982).
48. T. Kohonen, *Self-Organizing Maps*, (Springer, Berlin, Germany, 2001).
49. R. Caldas, Y. Hu, F. B. de Lima Neto, B. Markert, "Self-organizing maps and fuzzy C-means algorithms on gait analysis based on inertial sensors data" in *International Conference on Intelligent Systems Design and Applications*, A. M. Madureira, A. Abraham, D. Gamboa, P. Novais, Eds. (Advances in Intelligent Systems and Computing, Springer, Cham, Switzerland, 2017), Vol. vol. 557, pp. 197–205.
50. P. F. Lamb, A. Mündermann, R. M. Bartlett, A. Robins, Visualizing changes in lower body coordination with different types of foot orthoses using self-organizing maps (SOM). *Gait Posture* **34**, 485–489 (2011).
51. M. Dubey, A. K. Wadhwani, S. Wadhwani, Gait based vertical ground reaction force analysis for Parkinson's disease diagnosis using self organizing map. *Int. J. Adv. Biol. Biomed. Res.* **1**, 2322–4827 (2013).
52. M. Goethel, Biomechanical effects of the abductor hip muscles local fatigue. Figshare. https:/doi.org/10.6084/m9.figshare.12514289.v1. Deposited 24 July 2020.